

REPORT DOCUMENTATION PAGE				Form Approved OMB NO. 0704-0188	
<p>The public reporting burden for this collection of information is estimated to average 1 hour per response, including the time for reviewing instructions, searching existing data sources, gathering and maintaining the data needed, and completing and reviewing the collection of information. Send comments regarding this burden estimate or any other aspect of this collection of information, including suggestions for reducing this burden, to Washington Headquarters Services, Directorate for Information Operations and Reports, 1215 Jefferson Davis Highway, Suite 1204, Arlington VA, 22202-4302. Respondents should be aware that notwithstanding any other provision of law, no person shall be subject to any penalty for failing to comply with a collection of information if it does not display a currently valid OMB control number.</p> <p>PLEASE DO NOT RETURN YOUR FORM TO THE ABOVE ADDRESS.</p>					
1. REPORT DATE (DD-MM-YYYY)		2. REPORT TYPE New Reprint		3. DATES COVERED (From - To) -	
4. TITLE AND SUBTITLE 27Al, 47,49Ti, 31P, and 13C MAS NMR Study of VX, GD, and HD Reactions with Nanosize Al2O3, Conventional Al2O3 and TiO2, and Aluminum and Titanium Metal				5a. CONTRACT NUMBER W911NF-07-1-0053	
				5b. GRANT NUMBER	
				5c. PROGRAM ELEMENT NUMBER BD2256	
6. AUTHORS G.W. Wagner, L.R. Procell, S. Munavalli				5d. PROJECT NUMBER	
				5e. TASK NUMBER	
				5f. WORK UNIT NUMBER	
7. PERFORMING ORGANIZATION NAMES AND ADDRESSES New York Structural Biology RRL 317B 1275 York Ave. New York, NY 10021 -6094				8. PERFORMING ORGANIZATION REPORT NUMBER	
9. SPONSORING/MONITORING AGENCY NAME(S) AND ADDRESS(ES) U.S. Army Research Office P.O. Box 12211 Research Triangle Park, NC 27709-2211				10. SPONSOR/MONITOR'S ACRONYM(S) ARO	
				11. SPONSOR/MONITOR'S REPORT NUMBER(S) 51980-CH.2	
12. DISTRIBUTION AVAILABILITY STATEMENT Approved for public release; distribution is unlimited.					
13. SUPPLEMENTARY NOTES The views, opinions and/or findings contained in this report are those of the author(s) and should not be construed as an official Department of the Army position, policy or decision, unless so designated by other documentation.					
14. ABSTRACT Reactions of VX, GD, and HD with Al2O3, TiO2 (anatase and rutile), aluminum, and titanium metal powders have been studied by 27Al, 47,49Ti, 31P, and 13C MAS NMR. VX, GD, and HD hydrolyze on both nanosize and conventional Al2O3. A significant droplet size effect on the reaction kinetics is observed. For VX and GD, 27Al and 31P MAS NMR detect the formation of aluminum phosphonate complexes. Similarly, GD hydrolysis on TiO2 yields titanium phosphonate species as detected by 31P MAS NMR. Attempts at obtaining 47,49Ti NMR spectra of					
15. SUBJECT TERMS Nerve agent, VX, GD, HD, Anatase, Rutile, Decontamination, sorbent, 27Al, 47,49Ti, 31P, 13C MAS NMR					
16. SECURITY CLASSIFICATION OF:			17. LIMITATION OF ABSTRACT UU	15. NUMBER OF PAGES	19a. NAME OF RESPONSIBLE PERSON Michael Goger
a. REPORT UU	b. ABSTRACT UU	c. THIS PAGE UU			19b. TELEPHONE NUMBER 212-939-0660

## **Report Title**

**<sup>27</sup>Al, <sup>47,49</sup>Ti, <sup>31</sup>P, and <sup>13</sup>C MAS NMR Study of VX, GD, and HD Reactions with Nanosize Al<sub>2</sub>O<sub>3</sub>, Conventional Al<sub>2</sub>O<sub>3</sub> and TiO<sub>2</sub>, and Aluminum and Titanium Metal**

### **ABSTRACT**

Reactions of VX, GD, and HD with Al<sub>2</sub>O<sub>3</sub>, TiO<sub>2</sub> (anatase and rutile), aluminum, and titanium metal powders have been studied by <sup>27</sup>Al, <sup>47,49</sup>Ti, <sup>31</sup>P, and <sup>13</sup>C MAS NMR. VX, GD, and HD hydrolyze on both nanosize and conventional Al<sub>2</sub>O<sub>3</sub>. A significant droplet size effect on the reaction kinetics is observed. For VX and GD, <sup>27</sup>Al and <sup>31</sup>P MAS NMR detect the formation of aluminum phosphonate complexes. Similarly, GD hydrolysis on TiO<sub>2</sub> yields titanium phosphonate species as detected by <sup>31</sup>P MAS NMR. Attempts at obtaining <sup>47,49</sup>Ti NMR spectra of these species and those of titanium phosphonate model compounds at 14 T were marginally successful. <sup>47,49</sup>Ti NMR spectra were obtainable for anatase and titanium metal; thus, severe secondorder quadrupolar linebroadening is suspected for the titanium phosphonate complexes. <sup>47,49</sup>Ti NMR spectra obtained for anatase at high magnetic field (17.5 and 21 T) showed anticipated improvement in peak width and resolution. GD reacted with aluminum and titanium powder in the presence of water results in acid-dissolution of the metals and the formation of their respective metal phosphonates.



---

**REPORT DOCUMENTATION PAGE (SF298)**  
**(Continuation Sheet)**

---

Continuation for Block 13

ARO Report Number 51980.2-CH  
27Al, 47,49Ti, 31P, and 13C MAS NMR Study o ...

Block 13: Supplementary Note

© 2007 . Published in Journal of Physical Chemistry C, Vol. 111 (47) (2007), ( (47). DoD Components reserve a royalty-free, nonexclusive and irrevocable right to reproduce, publish, or otherwise use the work for Federal purposes, and to authorize others to do so (DODGARS §32.36). The views, opinions and/or findings contained in this report are those of the author(s) and should not be construed as an official Department of the Army position, policy or decision, unless so designated by other documentation.

Approved for public release; distribution is unlimited.

# <sup>27</sup>Al, <sup>47,49</sup>Ti, <sup>31</sup>P, and <sup>13</sup>C MAS NMR Study of VX, GD, and HD Reactions with Nanosize Al<sub>2</sub>O<sub>3</sub>, Conventional Al<sub>2</sub>O<sub>3</sub> and TiO<sub>2</sub>, and Aluminum and Titanium Metal

George W. Wagner,<sup>\*,†</sup> Lawrence R. Procell,<sup>†</sup> and Shekar Munavalli<sup>‡,§</sup>

U.S. Army Edgewood Chemical Biological Center, Aberdeen Proving Ground, Maryland 21010-5424, and GEO-CENTERS, Inc., Gunpowder Branch, P.O. Box 68, Aberdeen Proving Ground, Maryland 21010-0068

Received: June 11, 2007; In Final Form: September 18, 2007

Reactions of VX, GD, and HD with Al<sub>2</sub>O<sub>3</sub>, TiO<sub>2</sub> (anatase and rutile), aluminum, and titanium metal powders have been studied by <sup>27</sup>Al, <sup>47,49</sup>Ti, <sup>31</sup>P, and <sup>13</sup>C MAS NMR. VX, GD, and HD hydrolyze on both nanosize and conventional Al<sub>2</sub>O<sub>3</sub>. A significant droplet size effect on the reaction kinetics is observed. For VX and GD, <sup>27</sup>Al and <sup>31</sup>P MAS NMR detect the formation of aluminum phosphonate complexes. Similarly, GD hydrolysis on TiO<sub>2</sub> yields titanium phosphonate species as detected by <sup>31</sup>P MAS NMR. Attempts at obtaining <sup>47,49</sup>Ti NMR spectra of these species and those of titanium phosphonate model compounds at 14 T were marginally successful. <sup>47,49</sup>Ti NMR spectra were obtainable for anatase and titanium metal; thus, severe second-order quadrupolar linebroadening is suspected for the titanium phosphonate complexes. <sup>47,49</sup>Ti NMR spectra obtained for anatase at high magnetic field (17.5 and 21 T) showed anticipated improvement in peak width and resolution. GD reacted with aluminum and titanium powder in the presence of water results in acid-dissolution of the metals and the formation of their respective metal phosphonates.

## Introduction

Inorganic oxides are currently being considered as reactive sorbents for the decontamination of chemical warfare agents (CWA).<sup>1</sup> Indeed, an aluminum oxide-based sorbent has already been fielded for use on vehicles and soldiers' personal equipment. Another, potential application of reactive sorbents is in aircraft filtration systems to provide protection to occupants in contaminated environments. Besides metal oxides, the interaction of CWA with metals is also a concern in the demilitarization<sup>2</sup> of bulk CWA and CWA munitions, as many chemical neutralization and/or natural degradation products are acidic and extremely corrosive to processing equipment. Finally, the identification of stable, metal-derived CWA byproducts is of potential importance to the Chemical Weapons Convention Treaty,<sup>2</sup> where such materials may be uncovered during challenge inspections.

Previous work with nanosize aluminum oxide (AP-Al<sub>2</sub>O<sub>3</sub>)<sup>3</sup> assessed the reactions of GB (isopropyl methylphosphonofluoridate), GD (pinacolyl methylphosphonofluoridate), HD [bis-(2-chloroethyl) sulfide], and VX [O-ethyl S-(2-diisopropylamino)-ethyl methylphosphonothioate], where it was found that the products of the nerve agents GB, GD, and VX formed novel aluminophosphonate compounds. Also, appropriate aluminophosphonate "markers" possessing potential environmental stability were identified for each of these nerve agents. In the current study, conventional aluminum oxide (γ-Al<sub>2</sub>O<sub>3</sub>) is examined and compared to the previous AP-Al<sub>2</sub>O<sub>3</sub> results. Additionally, the reaction of GD with aluminum metal to form the anticipated aluminophosphonate is demonstrated. Also

described are preliminary assessments of GD reactions with titanium oxide and titanium metal.

## Experimental Section

**Materials.** The γ-alumina used is Selexsorb CDX (Alcoa) and has a surface area of 400 m<sup>2</sup>/g. The alumina was used as received. Anatase, rutile, aluminum, and titania metal powders, titanium(IV) isopropoxide, and pinacolyl methylphosphonate were all obtained from Aldrich. <sup>13</sup>C-labeled HD (HD\*), obtained locally, was employed to enhance sensitivity for <sup>13</sup>C NMR experiments.

**Titanophosphonate Synthesis.** Titanophosphonate synthesis was adapted from Mutin et al.<sup>4</sup> using titanium(IV) isopropoxide (TIP) and pinacolyl methylphosphonate (PMPA). Typically, a measured molar-amount of PMPA was predissolved in dried CH<sub>3</sub>CN (mol-sieves), to which was added a measured, molar-amount of TIP with stirring. <sup>1</sup>H and <sup>31</sup>P NMR were employed to determine the extent of reaction of TIP and PMPA, respectively, to form titanophosphonate species. In particular, it was found that a 1:2 molar ratio of TIP:PMPA gave an immediate white precipitate of compound **3** with complete reaction/complexation of TIP and PMPA. Recrystallization of this material with alcohol provided light-yellow, clear crystals which were apparently amorphous as they did not diffract X-rays. Calculated for C<sub>12</sub>H<sub>26</sub>O<sub>7</sub>P<sub>2</sub>Ti: C, 36.8; H, 6.7; P, 15.8; Ti, 12.2. Found: C, 35.90; H, 7.19; P, 11.67; Ti, 13.39.

**NMR.** <sup>27</sup>Al, <sup>31</sup>P, and <sup>13</sup>C MAS NMR spectra were obtained at 7 T with a Varian Unityplus 300 NMR spectrometer equipped with a Doty Scientific 7 mm high-speed VT-MAS probe.<sup>47,49</sup> <sup>13</sup>C MAS NMR spectra were obtained at 14, 17.5, and 21 T with Varian INOVA 600 and Bruker AVANCE 750 and 900 NMR spectrometers, respectively, using spin echo pulse sequences to minimize "ringing".<sup>5</sup> The 14 and 17.5 T instruments were equipped with Doty Scientific 5 mm XC MAS NMR probes, and the 21 T instrument was equipped with a Bruker 3.2 mm MAS NMR probe. Double O-ring caps were used to seal 7 mm

\* To whom correspondence should be addressed. Tel: (410) 436-8468. E-mail: george.wagner@us.army.mil.

† U.S. Army Edgewood Chemical Biological Center.

‡ GEO-CENTERS, Inc..

§ Current address: SAIC, Gunpowder Branch, P.O. Box 68, APG, MD 21010-0068.

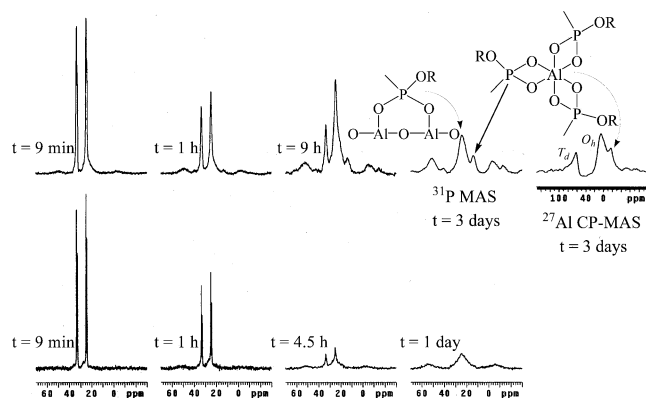


**Figure 1.** Selected  $^{31}\text{P}$  MAS and  $^{27}\text{Al}$  CP-MAS NMR spectra obtained at 7.0 T for 16  $\mu\text{L}$  GD on  $\gamma\text{-Al}_2\text{O}_3$  (top spectra) and  $^{31}\text{P}$  MAS NMR spectra for 3  $\mu\text{L}$  GD on AP- $\text{Al}_2\text{O}_3$  (bottom spectra) at the indicated times. Insets show assignments of surface-bound PMPA, its corresponding aluminophosphonate **1**, and  $T_d$  and  $O_h$  sites of  $\gamma\text{-Al}_2\text{O}_3$  (see text).

and 5 mm rotors (Doty Scientific) containing agent-contaminated samples. Normal “press-fit” caps were used on 5 (Doty Scientific) and 3.2 mm (Bruker) rotors containing the anatase samples. Direct polarization (DP) was used to obtain most MAS NMR spectra [i.e., no cross-polarization (CP) was used]; however,  $^{27}\text{Al}$  CP-MAS NMR was employed to detect the GD-derived aluminophosphonate **1** on  $\gamma\text{-Al}_2\text{O}_3$  as previously described.<sup>3</sup> External shift references used for  $^{27}\text{Al}$ ,  $^{31}\text{P}$ ,  $^{13}\text{C}$ , and  $^{47,49}\text{Ti}$  were 0.1 M  $\text{Al}(\text{NO}_3)_3 \cdot 9\text{H}_2\text{O}$  (0 ppm), 85%  $\text{H}_3\text{PO}_4$  (0 ppm), TMS (0 ppm), and  $\text{SrTiO}_3$  (−843 ppm<sup>5</sup>), respectively.

**Reaction Procedure.** *Caution.* These experiments should only be performed by trained personnel using applicable safety procedures. In a typical kinetic run with  $\gamma\text{-Al}_2\text{O}_3$ , single 3.5- $\mu\text{L}$  drops (ca. 1.5 wt %) or larger 13–16  $\mu\text{L}$  drops (ca. 5 wt %) of neat, liquid agent were added via syringe to the center of a column contained in a 7 mm MAS NMR rotor. The rotor was then sealed with a double O-ring cap. MAS NMR spectra were obtained periodically to monitor the reaction in situ. For the very high loadings of GD examined on titania, titanium, and aluminum metal, the agent was either mixed with the material prior to NMR analysis or allowed to settle onto a short column of the material contained in a 5 mm NMR tube. The tube was then capped, sealed with Parafilm, and placed within the NMR spectrometer such that the entire column of material/sorbed agent was contained within the NMR detector-coil region. This latter procedure similarly allowed in situ NMR monitoring of reactions with these solid materials using “solution” NMR conditions.

## Results and Discussion

### Conventional vs Nanosize Aluminum Oxide Reactions.

Figures 1–3 show MAS NMR spectra obtained for GD, VX, and HD reacted with conventional  $\gamma\text{-Al}_2\text{O}_3$ , showing the effect of droplet size on reaction rate. Corresponding reaction profiles are shown in Figure 4. For comparison, previous data<sup>3</sup> is also shown for GD, VX, and HD on nanosize AP- $\text{Al}_2\text{O}_3$ .

For GD, an identical rate ( $t_{1/2} = 1.8$  h), regardless of drop size (3 or 16- $\mu\text{L}$ ), is observed for  $\gamma\text{-Al}_2\text{O}_3$  and AP- $\text{Al}_2\text{O}_3$ . The expected<sup>3</sup> GD-derived aluminophosphonate ( $\text{Al}[\text{O}_2\text{P}(\text{CH}_3)\text{-OPin}]_3$ , **1**) is also clearly evident in both the  $^{31}\text{P}$  MAS and  $^{27}\text{Al}$  CP-MAS NMR spectra as indicated in Figure 1. Other peaks are due to surface-bound PMPA<sup>3</sup> ( $^{31}\text{P}$ ) and tetrahedral ( $T_d$ ) and octahedral ( $O_h$ ) Al sites  $\gamma\text{-Al}_2\text{O}_3$  ( $^{27}\text{Al}$ ).<sup>6</sup>

As depicted in Figure 1, the Al site for compound **1** is envisioned to possess  $O_h$  symmetry owing to the proximity of

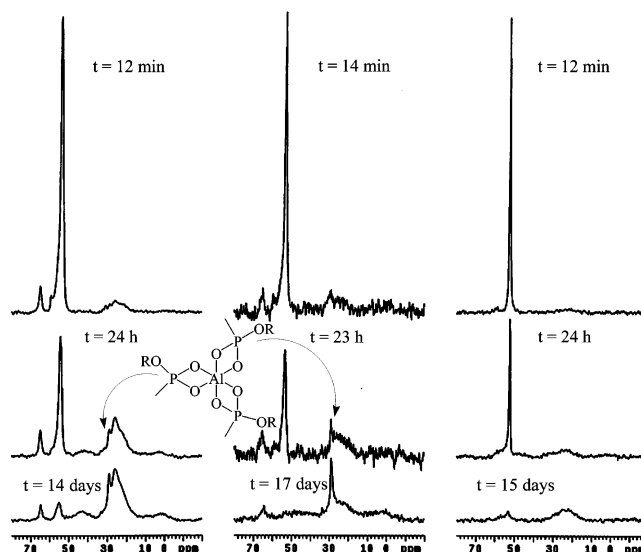


**Figure 2.** Selected  $^{31}\text{P}$  MAS NMR spectra obtained for 15  $\mu\text{L}$  VX on  $\gamma\text{-Al}_2\text{O}_3$  (left column), 3.5  $\mu\text{L}$  VX on  $\gamma\text{-Al}_2\text{O}_3$  (middle column), and 3.5  $\mu\text{L}$  VX on AP- $\text{Al}_2\text{O}_3$  (right column) at the indicated times. Inset shows peaks for aluminophosphonate **2** (see text).

its  $^{27}\text{Al}$  MAS NMR peak to that of the  $O_h$  peak<sup>6</sup> for  $\gamma\text{-Al}_2\text{O}_3$ . The ability to adequately resolve these two, distinct  $O_h$  sites is due to two, main favorable factors that lead to reduced second-order quadrupole effects.<sup>7,8</sup> The first is that, even though  $^{27}\text{Al}$  is quadrupolar, it possesses a modest quadrupole moment,  $Q$  (Table 1), meaning that it will only modestly couple with nonzero electric field gradients,  $eq$ .<sup>8</sup> Second, symmetric environments such as  $O_h$  and the like, even though perhaps slightly perturbed, provide for a nearly zero electric field gradient and, hence, a nearly zero quadrupole coupling constant,  $Q_{cc} = e^2Qq/h$ . Thus, even at a modest field of 7.0 T, relatively narrow NMR linewidths and adequate resolution of various  $^{27}\text{Al}$  sites is possible for alumina/aluminophosphonate mixtures. Unfortunately, as will be seen below, conditions are not quite so favorable for various  $^{47,49}\text{Ti}$  sites in titania/titanophosphonate mixtures.

Regarding the reaction profiles for VX in Figure 4, there is some dependence of the steady-state reaction rate on droplet size as the 3.5- $\mu\text{L}$  droplets possess nearly identical half-lives on both  $\gamma\text{-Al}_2\text{O}_3$  and AP- $\text{Al}_2\text{O}_3$ ,  $t_{1/2} = 6.8$  and 6.4 days, respectively, yet the larger 15- $\mu\text{L}$  droplet size on  $\gamma\text{-Al}_2\text{O}_3$  yields  $t_{1/2} = 9.2$  days.

Analogous to the GD reaction, the VX-derived aluminophosphonate ( $\text{Al}[\text{O}_2\text{P}(\text{CH}_3)\text{OEt}]_3$ , **2**) forms as indicated in the  $^{31}\text{P}$  MAS NMR spectra of Figure 2. Further note the sharpness of the  $^{31}\text{P}$  MAS NMR peak for this species, which remains soluble near neutral pH,<sup>3</sup> compared to that of **1** which is insoluble at neutral pH. Thus, the sharpness of the peak for **2** is attributed to increased motion as a result of this species remaining dissolved within the adsorbed water layer residing on the as-received (un-dried)  $\gamma\text{-Al}_2\text{O}_3$ .

For HD, the dependence of steady-state reaction rate on droplet size is quite extreme, with the 13- $\mu\text{L}$  droplet size exhibiting  $t_{1/2} = 70.9$  h, compared to 44 min for the 3.5- $\mu\text{L}$  droplet. For the small 3.5- $\mu\text{L}$  droplet size, the reaction rate on  $\gamma\text{-Al}_2\text{O}_3$  is considerably faster than that on AP- $\text{Al}_2\text{O}_3$  ( $t_{1/2} = 6.3$  h). However, the surface hydration state, which was not controlled, may be contributing substantially to this difference. Dramatic effects of surface hydration on HD reaction kinetics on sorbents have been previously observed.<sup>9</sup> Indeed, substantial formation of the CH-TG sulfonium ion<sup>9</sup> on  $\gamma\text{-Al}_2\text{O}_3$  indicates

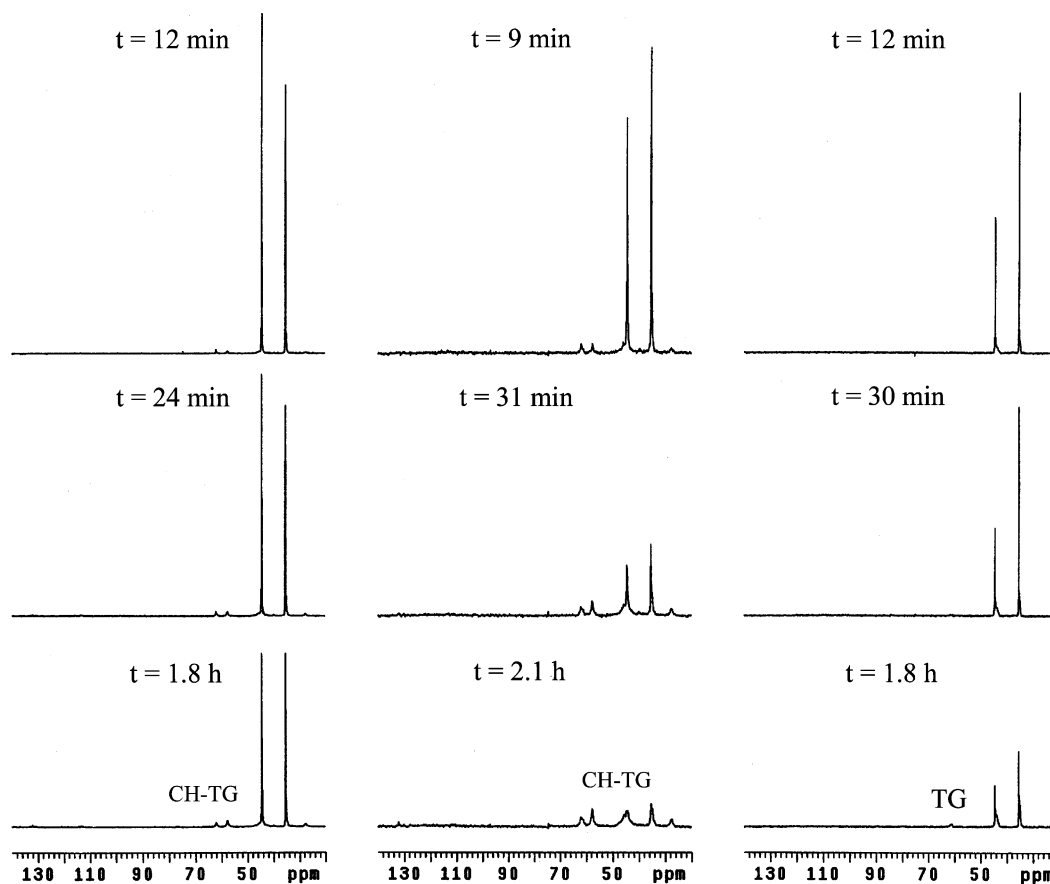


**Figure 3.** Selected  $^{13}\text{C}$  MAS NMR spectra obtained for  $\mu\text{L HD}^*$  on  $\gamma\text{-Al}_2\text{O}_3$  (left column),  $3.5 \mu\text{L HD}^*$  on  $\gamma\text{-Al}_2\text{O}_3$  (middle column), and  $3.5 \mu\text{L HD}^*$  on  $\text{AP-Al}_2\text{O}_3$  (right column) at the indicated times. Insets show peaks detected for CH-TG sulfonium ion and TG hydrolysis products (see text).

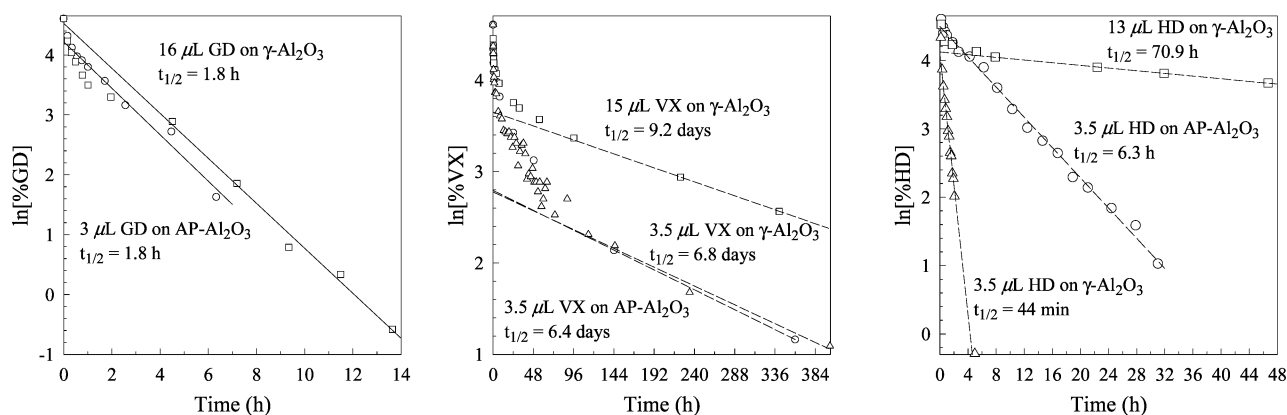


**Figure 4.** Reaction profiles for GD, VX, and HD reactions with  $\gamma\text{-Al}_2\text{O}_3$  and  $\text{AP-Al}_2\text{O}_3$ .

**TABLE 1: NMR Parameters<sup>a</sup> for  $^{27}\text{Al}$ ,  $^{47}\text{Ti}$ , and  $^{49}\text{Ti}$**

nuclide	natural abund (%)	$\nu_0$ (MHz) <sup>b</sup>	$I$	$Q$ (barn)
$^{27}\text{Al}$	100	156.3	5/2	0.15
$^{47}\text{Ti}$	7.28	33.8	5/2	0.29
$^{49}\text{Ti}$	5.51	33.8	7/2	0.24

<sup>a</sup> Reference 8. <sup>b</sup> Resonance frequency,  $\nu_0$ , at 14.1 T.

abundant water is present; alternatively, the preferred thiodiglycol (TG) product observed for  $\text{AP-Al}_2\text{O}_3$  is suggestive of a much drier surface. Additional studies looking at hydration effects must be conducted to definitively compare the relative reactivities of the two aluminas.

The reactivity behavior exhibited by the agents, which is drop size-dependent in some cases, may be attributed to three major effects: (1) smaller drops react faster owing to their large surface

to volume ratio; (2) the vapor pressure of the agents varies widely,<sup>10</sup> with  $\text{GD} > \text{HD} \gg \text{VX}$ , allowing the more volatile agents to spread more rapidly through the sorbent (in lieu of other transport mechanisms such as water-solubility); and (3) the order of water solubility of the agents, under basic conditions, is  $\text{GD} > \text{VX} \gg \text{HD}$ . Thus, with its solubility in water, GD is able to spread and react more quickly across the hydrated alumina surface and drop size has little effect; the high volatility of GD also contributes to its ability to quickly disperse and react. However, VX has more limited water solubility (under basic conditions;<sup>1</sup>  $\text{p}K_a = 8.6^{11}$ ) and extremely low volatility; thus, it spreads more slowly, even on a (basic) hydrated surface, resulting in a noticeable drop-size effect, and it is by far the most persistent. Finally, although HD is water-insoluble, its volatility and rather facile hydrolysis<sup>1</sup> still enables it react quite

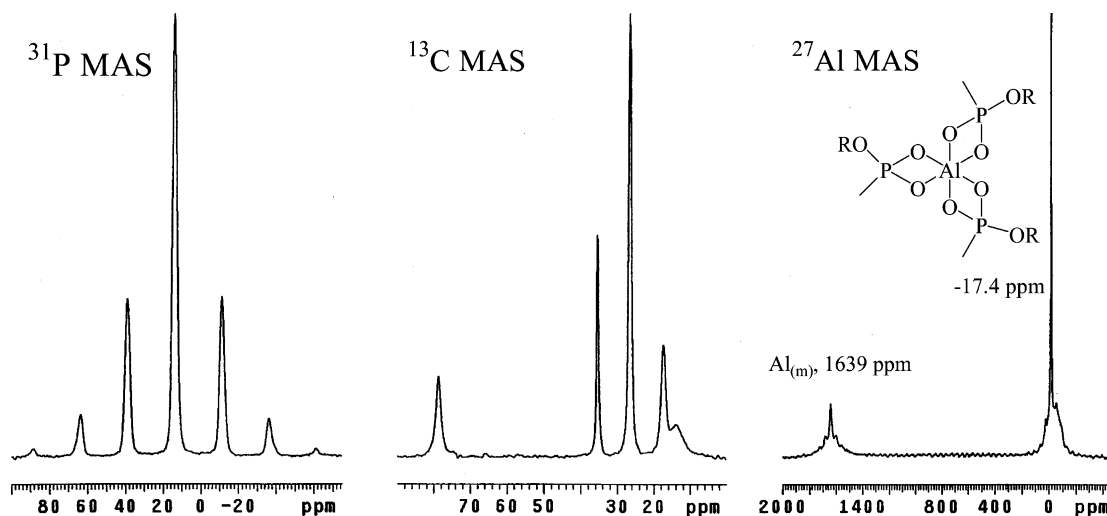


**Figure 5.** <sup>31</sup>P, <sup>13</sup>C, and <sup>27</sup>Al MAS NMR spectra obtained at 7.0 T for GD reacted with Al<sub>(m)</sub> in the presence of water. Insets show assignments of peaks to Al<sub>(m)</sub> and aluminophosphonate **1** (see text).

fast in small drops but much more slowly in large drops. Additionally, surface hydration has been shown to have a profound impact on the reaction of HD<sup>9</sup> (as well as the other agents; see below for GD), and future studies are needed to sort this out. Indeed, such uncontrolled hydration effects could well account for the apparent reactivity differences exhibited by γ-Al<sub>2</sub>O<sub>3</sub> and AP-Al<sub>2</sub>O<sub>3</sub> in the small, 3.5-μL drop-size experiments for HD.

**GD Reaction With Al Metal.** As mentioned above, nerve agent degradation generates acidic products which have been shown<sup>3</sup> to dissolve alumina to generate aluminophosphonates. Such acids would also be expected to oxidize/corrode aluminum metal (Al<sub>(m)</sub>) to generate the same products. The reaction of GD with Al<sub>(m)</sub> powder in the presence of water does result in the quantitative formation of **1**, a white, microcrystalline powder (Figure 5). Note that a single <sup>31</sup>P MAS NMR peak is present for the compound indicative of the simple crystal structure containing only a single P site. The <sup>13</sup>C MAS NMR spectrum yields additional important information on the structure, showing that the pinacolyl group is still attached to the phosphonate; that is, secondary hydrolysis of this group did not occur. Finally, the <sup>27</sup>Al MAS NMR spectrum shows residual Al<sub>(m)</sub> at the expected Knight shift of 1640 ppm.<sup>12</sup> Note that this metal has cubic symmetry and, hence, an essentially zero *Q*<sub>cc</sub>, leading to its quite narrow NMR line width.

**Titanium Oxide Reactions.** Titanium oxide exists in two common forms, rutile and anatase.<sup>13</sup> Initial work focused on their relative reactivities for GD and the potential formation of titanophosphonates.<sup>4</sup> Figure 6 shows <sup>31</sup>P NMR spectra obtained for 50 wt % GD on anatase (loaded with 11 wt % water) and rutile (initially without added water). In the absence of added water, GD reacts only slowly on rutile; however, the addition of copious water (100 wt %) results in the facile, quantitative reaction to the expected hydrolysis product PMPA. For GD on anatase with preadsorbed water, a rather facile reaction similarly ensues, again providing quantitative conversion to PMPA. Thus, both anatase and rutile react with GD, provided adequate water is present.

Closer inspection of the GD-anatase product by <sup>31</sup>P MAS NMR (Figure 6), which enabled improved resolution, revealed additional, small peaks due to titanophosphonate species, at least some of which are soluble as shown in the <sup>31</sup>P NMR spectrum of the CH<sub>3</sub>CN extract of the product(s) (Figure 6). The large peak in the extract is free PMPA; the small peaks are due to

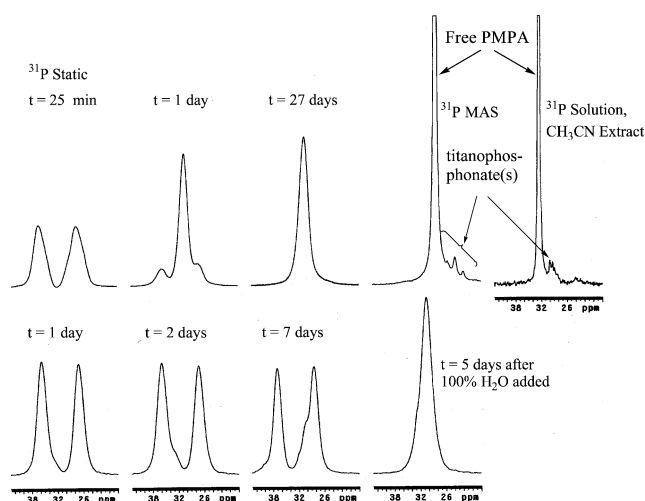


**Figure 6.** Selected <sup>31</sup>P and <sup>31</sup>P MAS NMR spectra obtained for GD reactions with anatase (11 wt % water added; top spectra) and rutile (bottom spectra; before and after 100 wt % water added).

PMPA complexed in one or more titanophosphonate species. Unlike the corresponding aluminophosphonate, the titanophosphonate(s) must possess a more complex structure as evidenced by the multiple P sites.

As shown in Figure 7, attempts at synthesizing<sup>4</sup> the authentic titanophosphonate(s) starting with Ti(OPr<sup>i</sup>)<sub>4</sub> (TIP) and PMPA showed that a mole ratio of about one Ti<sup>4+</sup> to four PMPA gave a soluble complex possessing multiple P sites (a minor amount of free PMPA is also detected). However, a mole ratio of one Ti<sup>4+</sup> to two PMPA gave an immediate white precipitate of **3** with no free PMPA. <sup>31</sup>P MAS NMR showed the presence of multiple P sites for **3**. <sup>13</sup>C MAS NMR confirmed that the PMPA remained intact in the complex (no hydrolysis of the pinacolyl group occurred). An attempt at obtaining a <sup>47,49</sup>Ti NMR<sup>5,13–14</sup> spectrum of the compound yielded only a single, broad feature at −512 ppm. Such a broad peak suggests that the Ti sites possess distorted symmetry and, hence, a large *Q*<sub>cc</sub>.

**GD Reaction With Ti Metal.** Figure 8 shows NMR spectra obtained for the reaction for GD with titanium metal powder (Ti<sub>(m)</sub>). For this sample, Ti<sub>(m)</sub> (0.1 g, 2.1 mmol) was mixed with anatase (0.3 g, 3.8 mmol) and reacted with 193 wt % GD (0.77 mL, 4.2 mmol). <sup>31</sup>P NMR of the precipitate in contact with the reaction solution (Figure 8) showed the formation of the



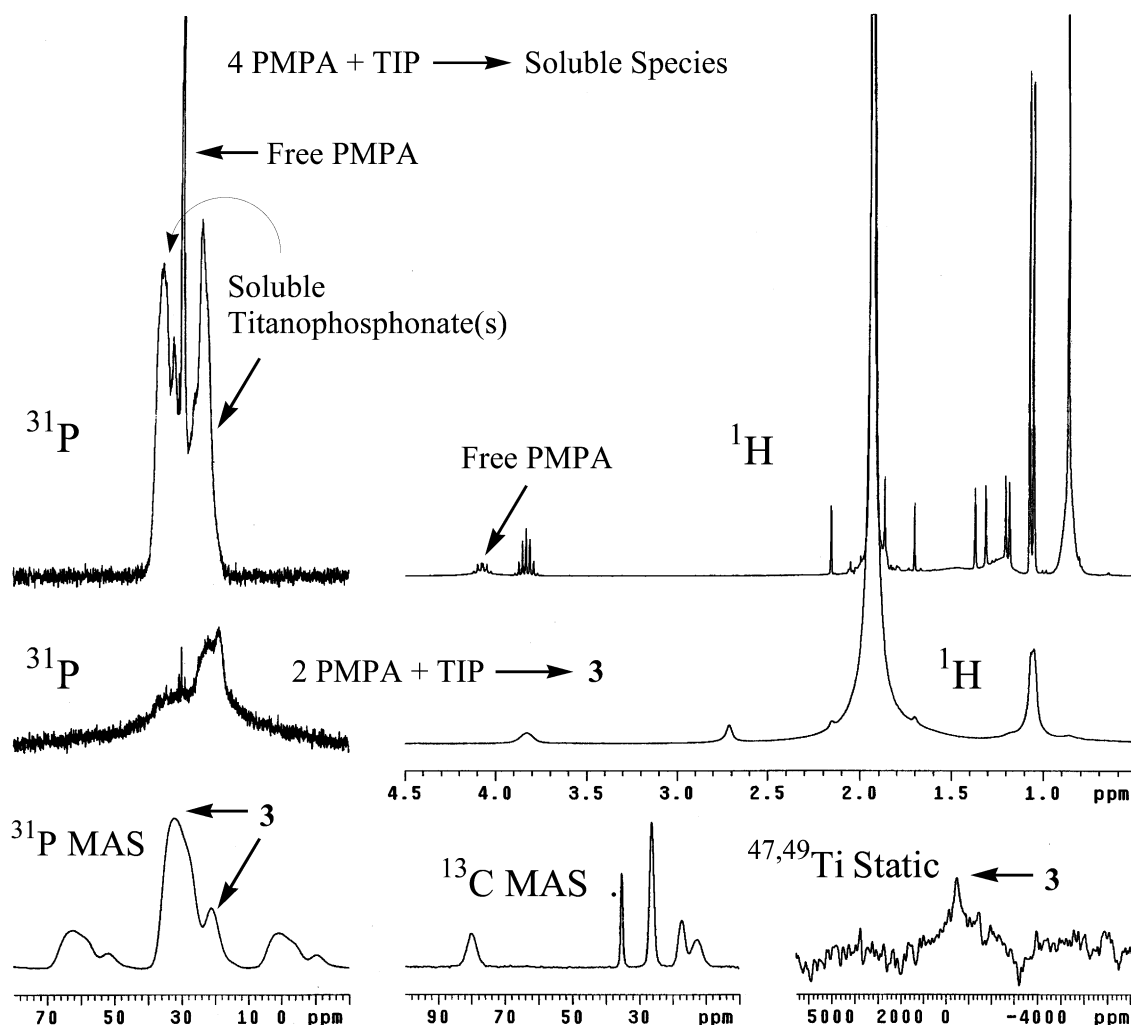


**Figure 7.**  $^{31}\text{P}$  and  $^1\text{H}$  solution NMR,  $^{47,49}\text{Ti}$  static NMR, and  $^{31}\text{P}$  and  $^{13}\text{C}$  MAS NMR spectra obtained at 7.0 T and 14 T ( $^{47,49}\text{T}$ ) for titanophosphonate syntheses. Insets show PMPA:TIP ratios employed and peaks due to soluble titanophosphonate(s), free PMPA, and insoluble titanophosphonate 3 (see text).

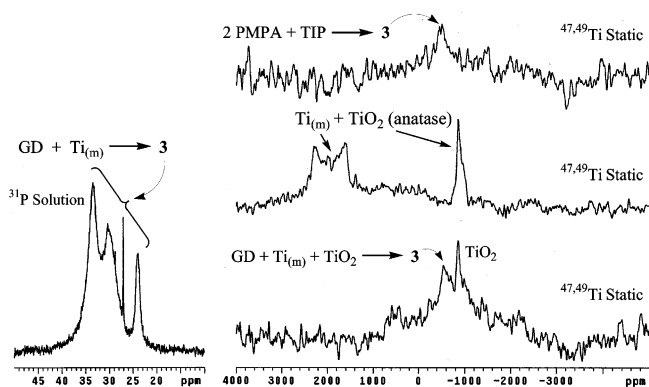


**Figure 8.**  $^{31}\text{P}$  solution NMR spectrum obtained for GD reacted with  $\text{Ti}_{(\text{m})}$  (left) and  $^{47,49}\text{Ti}$  static NMR spectra obtained at 14 T for the reaction of GD with  $\text{Ti}_{(\text{m})}$  mixed with anatase (right column):  $\text{Ti}_{(\text{m})}$  mixed with anatase before (middle right) and after GD added (bottom right). Also shown is the  $^{47,49}\text{Ti}$  static NMR spectrum of authentic 3 synthesized from 2:1 reaction of PMPA and TIP (top, right). Insets show reactions involved and peak assignments for titanophosphonate 3,  $\text{Ti}_{(\text{m})}$  and anatase (see text).

titanophosphonate species with very little free PMPA (sharp peak).  $^{47,49}\text{Ti}$  NMR spectra taken before and after the addition of GD show the loss of the  $\text{Ti}_{(\text{m})}$  peak (at the expected Knight shift<sup>13b,14</sup> of ca. 2800 ppm) and the formation of the titanophosphonate feature at  $-547$  ppm. The anatase peak at  $-862$

ppm also exhibited a substantial decrease, showing that GD reacted with this material as well. Note that  $\text{Ti}_{(\text{m})}$  possesses lower, hexagonal symmetry leading to a rather large  $Q_{\text{cc}}$  of 9.25 MHz<sup>13b</sup> and the resultant broadened line shape. By comparison, anatase possesses tetragonal symmetry leading to distorted  $O_h$  sites but a more modest  $Q_{\text{cc}}$  of 4.79 MHz<sup>13b</sup> and a much narrower line width. Note that for these low signal-to-noise spectra, only the  $^{49}\text{Ti}$  line is observed which is much sharper than the  $^{47}\text{Ti}$  line (see below) owing to its lower  $Q$  and larger spin<sup>5</sup> (Table 1).

#### Nature of the GD-Derived Titanophosphonate Structure.

Titanophosphonates are well-known in the literature,<sup>4,15</sup> many of which are soluble.<sup>4</sup> All exhibit quite complex, cage-like structures,<sup>16</sup> possessing multiple Ti and/or P sites. Furthermore, frequently the Ti sites are not symmetric. Thus, it is not surprising that the structure of the GD-derived titanophosphonate is also complex, possessing multiple P sites (as shown by  $^{31}\text{P}$  NMR) and that the Ti sites have apparent distorted symmetries (as suggested by  $^{47,49}\text{Ti}$  NMR). During synthesis from titanium alkoxides such as TIP, titanophosphonates tend to form Ti—O—Ti bonds in addition to Ti—O—P bonds.<sup>4</sup> This is due to a side reaction with adventitious water. Indeed, greater yields of titanophosphonates are seen with the addition of water.<sup>4</sup> Also, structures formed from bidentate ligands such as PMPA tend to form distorted D4R structures<sup>16</sup> containing a  $\text{Ti}_4\text{O}_4$  core.<sup>4b,15b</sup>

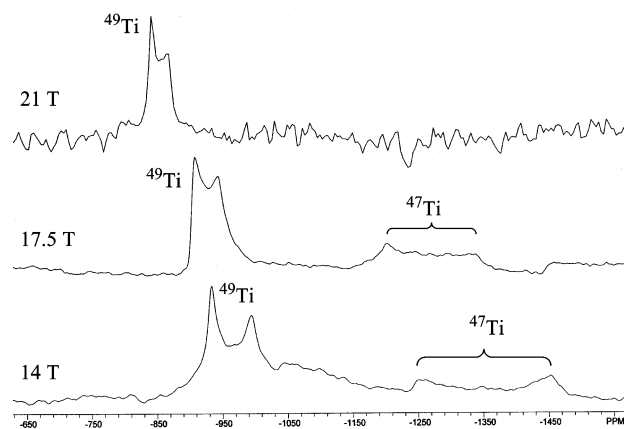


**Figure 9.**  $^{47,49}\text{Ti}$  MAS NMR spectra obtained for anatase at 14, 17.5, and 21 T. Insets show assignments of  $^{49}\text{Ti}$  and  $^{47}\text{Ti}$  nuclides (see text).

Thus, insoluble, 1:2 TIP:MPA titanophosphonate **3** is postulated to have the following empirical formula:  $\text{Ti}(\text{O})[\text{O}_2\text{P}(\text{CH}_3)\text{-OPin}]_2$ . Note that elemental analysis of the compound is consistent with this formula (see the Experimental Section).

**$^{47,49}\text{Ti}$  NMR at High Magnetic Field.** The attempts to obtain decent  $^{47,49}\text{Ti}$  NMR spectra of titanophosphonates at the modest field of 14 T, which was intended to both garner structural information analogous to that provided by the  $^{27}\text{Al}$  NMR spectra obtained for the aluminophosphonates (at a quite modest field of 7 T) and to provide for the in situ detection of these species within solid matrices, were only marginally successful. A major source of the difficulty apparently lies in the rather large  $Q$ 's of the  $^{47}\text{Ti}$  and  $^{49}\text{Ti}$  nuclei, 0.29 and 0.24, respectively (Table 1). Both of these  $Q$  values are considerably larger than that of  $^{27}\text{Al}$  (0.15). As mentioned earlier, large  $Q$  values lead to strong coupling to nonzero electric field gradients,  $eq$ , induced by distorted site symmetries giving rise to large quadrupole coupling constants,  $e^2qQ/h$ . Thus, the resultant large, second-order quadrupolar effects yield broadened lines and poor resolution of potential multiple site resonances. Indeed, it is precisely the severely distorted site symmetry suspected for the more complex titanophosphonates (see above) that appears to be particularly problematic since adequate spectra could be obtained for both  $\text{Ti}_{(m)}$  and anatase which possess modest symmetry perturbations ( $Q_{cc}$ 's of 9.25 and 4.79 MHz, respectively). Therefore, it is anticipated that **3** possesses a significantly larger  $Q_{cc}$ . Fortunately, such second-order quadrupole effects become less important and are relatively minimized at higher magnetic fields,<sup>7</sup> thus providing for relatively narrower lines and improved resolution. To investigate the potential advantage of obtaining  $^{47,49}\text{Ti}$  NMR spectra at higher magnetic fields, spectra of anatase were obtained at 17.5 and 21 T for comparison with results at 14 T. These spectra are shown in Figure 9.

The spectrum obtained at 14 T (bottom of Figure 9) shows a rather sharp, doublet-like pattern for the  $^{49}\text{Ti}$  nuclide centered at about  $-950$  ppm and a much broader feature for the  $^{47}\text{Ti}$  nuclide centered at  $-1350$  ppm. Although both nuclides are experiencing the same distorted  $O_h$  site symmetry and attendant nonzero electric field gradient,  $eq$ , the  $^{47}\text{Ti}$  nuclide exhibits more severe second-order quadrupole effects owing to both its larger  $Q$  (0.29 vs 0.24 for  $^{49}\text{Ti}$ ) and smaller spin ( $I = 5/2$  vs  $7/2$  for  $^{49}\text{Ti}$ ).<sup>5</sup> Thus, these seemingly subtle differences combine to make a dramatic impact on line width and resolution. At the higher magnetic fields, the expected line-narrowing and improved resolution is realized owing to the increasing dominance of the magnetic Zeeman interaction compared to that of the magnetic field-independent quadrupolar interaction<sup>7</sup> (the 21 T spectrum

does not possess adequate signal-to-noise to reveal the  $^{47}\text{Ti}$  resonance). Further note that the centers of the  $^{49}\text{Ti}$  and  $^{47}\text{Ti}$  features shift toward higher frequency<sup>5,7</sup> at the higher fields since these lineshapes are actually MAS-averaged second-order quadrupolar powder patterns and, thus, do not truly represent isotropic chemical shifts.

## Conclusions

Drop size has a large effect on the reaction of VX and HD with alumina but less effect on the reaction of GD. This is attributed to the both the greater water solubility and volatility of GD, which allows it to spread more readily over the hydrated alumina surface. GD reacts with  $\text{Al}_{(m)}$  to form the same aluminophosphonate **1** derived from alumina. GD reacts with rutile, anatase, and  $\text{Ti}_{(m)}$  to yield titanophosphonates. The formula of the insoluble GD-derived titanophosphonate **3** is postulated to be  $\text{Ti}(\text{O})[\text{O}_2\text{P}(\text{CH}_3)\text{OPin}]_2$ , in agreement with elemental analysis. High-field  $^{47,49}\text{Ti}$  MAS NMR of anatase shows marked narrowing of its signals compared to low-field measurements. High-field  $^{47,49}\text{Ti}$  MAS NMR should similarly allow for improved characterization of agent-derived titanophosphonates.

**Acknowledgment.** We acknowledge support of the work performed at NYSBC under U.S. Department of Defense Contract DAAD1902-1-0369. We thank Dr. B. Itin and Prof. A. Jerschow at New York Structural Biology Center for help with the high-field  $^{47,49}\text{Ti}$  NMR work. Prof. Jerschow, NYU, is a member of NYSBC. The Center is a STAR center supported by the New York State Office of Science, Technology, and Academic Research. We also thank Prof. A. L. Rhinegold, formerly at the University of Delaware, for X-ray examination of crystals of **3**.

## References and Notes

- (1) Yang, Y.-C.; Baker, J. A.; Ward, J. R. *Chem. Rev.* **1992**, 92, 1729–1743.
- (2) Yang, Y.-C. *Acc. Chem. Res.* **1999**, 32, 109–115 and references therein.
- (3) Wagner, G. W.; Procell, L. R.; O'Connor, R. J.; Munavalli, S.; Carnes, C. L.; Kapoor, P. N.; Klabunde, K. J. *J. Am. Chem. Soc.* **2001**, 123, 1636–1644.
- (4) (a) Mehring, M.; Guerrero, G.; Dahan, F.; Mutin, P. H.; Vioux, A. *Inorg. Chem.* **2000**, 39, 3325–3332. (b) Guerrero, G.; Mehring, M.; Mutin, P. H.; Dahan, F.; Vioux, A. *J. Chem. Soc., Dalton Trans.* **1999**, 1537–1538.
- (5) Dec, S. F.; Davis, M. F.; Maciel, G. E.; Bronnimann, C. E.; Fitzgerald, J. J.; Han, S.-S. *Inorg. Chem.* **1993**, 32, 955–959.
- (6) Huggins, B. A.; Ellis, P. D. *J. Am. Chem. Soc.* **1992**, 114, 2098–2108.
- (7) Gan, Z.; Gor'kov, P.; Cross, T. A.; Samoson, A.; Massiot, D. *J. Am. Chem. Soc.* **2002**, 124, 5634–5635.
- (8) Harris, R. K. *Nuclear Magnetic Resonance Spectroscopy*; Pitman: London, 1983; Chapter 5B.
- (9) (a) Wagner, G. W.; MacIver, B. K. *Langmuir* **1998**, 14, 6930–6934. (b) Wagner, G. W.; Koper, O.; Lucas, E.; Decker, S.; Klabunde, K. J. *J. Phys. Chem. B* **2000**, 104, 5118–5123.
- (10) Wagner, G. W.; Bartram, P. W.; Koper, O.; Klabunde, K. J. *J. Phys. Chem. B* **1999**, 103, 3225–3228.
- (11) Yang, Y.-C.; Szafraniec, L. L.; Beaudry, W. T.; Rohrbach, D. K.; Procell, L. R.; Samuel, J. B. *J. Org. Chem.* **1996**, 61, 8407–8413.
- (12) Andrew, E. R.; Hinshaw, W. S.; Tiffen, R. S. *J. Magn. Reson.* **1974**, 15, 191–195.
- (13) (a) Labouriau, A.; Earl, W. L. *Chem. Phys. Lett.* **1997**, 270, 278–284. (b) Bastow, T. J. *Z. Naturforsch.* **2000**, 55 a, 291–297.
- (14) Narath, A. *Phys. Rev.* **1967**, 162, 320–332.
- (15) (a) Walawalkar, M. G.; Horchler, S.; Dietrich, S.; Chakraborty, D.; Roesky, H. W.; Schäfer, M.; Schmidt, H.-G.; Sheldrick, G. M.; Murugavel, R. *Organometallics* **1998**, 17, 2865–2868. (b) Thora, D. L.; Harlow, R. L. *Inorg. Chem.* **1992**, 31, 3917–3923.
- (16) Walawalkar, M. G.; Roesky, H. W.; Murugavel, R. *Acc. Chem. Res.* **1999**, 32, 117–126.